

Origin of ultraviolet photoluminescence in ZnO quantum dots: Confined excitons versus surface-bound impurity exciton complexes

Vladimir A. Fonoberov and Alexander A. Balandin^{a)}

Nano-Device Laboratory, Department of Electrical Engineering, University of California-Riverside, Riverside, California 92521

(Received 16 June 2004; accepted 20 October 2004)

We have theoretically investigated the origin of ultraviolet photoluminescence (PL) in ZnO quantum dots with diameters from 2 to 6 nm. Two possible sources of ultraviolet PL have been considered: excitons confined in the quantum dot and excitons bound to an ionized impurity located at the quantum-dot surface. It is found that depending on the fabrication method and surface passivation technique, the ultraviolet PL of ZnO quantum dots can be attributed to either confined excitons or surface-bound ionized *acceptor*-exciton complexes. The exciton radiative lifetime is shown to be very sensitive to the exciton localization and can be used as a tool to discriminate between these two sources of PL. © 2004 American Institute of Physics. [DOI: 10.1063/1.1835992]

Zinc oxide (ZnO) has recently attracted significant attention as an efficient material for applications in UV light-emitting diodes, laser diodes, varistors, and transparent conducting films. Compared to other wide band-gap materials, ZnO has a very large exciton binding energy (~ 60 meV), which results in more efficient excitonic emission at room temperature. It is well known that semiconductor nanocrystals or quantum dots (QDs) may have superior optical properties than bulk crystals owing to quantum confinement effects. For example, Guo *et al.*¹ experimentally established that the third-order nonlinear susceptibility of ZnO nanoparticles is ~ 500 larger than that of bulk ZnO. Lately, there have been a number of reports of fabrication, structural, and optical characterization of ZnO QDs.^{1–8} Different fabrication techniques^{4,5} and methods of the QD surface modification^{1,8} have been used to quench the defect-related green photoluminescence and enhance the UV emission from ZnO QDs. However, the nature of the UV photoluminescence from ZnO QDs itself is not fully understood. Some authors attribute the UV photoluminescence to the recombination of confined excitons,² while others argue that the emission comes from surface impurities or defects.¹

Understanding the origin of UV photoluminescence in ZnO QDs is important from both fundamental science and proposed optoelectronic applications points of view. In this letter we address this issue by examining theoretically the optical properties of ZnO QDs with and without ionized impurities at the QD surface. We limit our consideration to spherical QDs with diameters in the range from 2 to 6 nm, because common fabrication techniques^{1–8} give nearly spherical ZnO QDs with diameter less than 10 nm.

There are only a few reports on the calculation of exciton states in the presence of charges at the QD surface. Using the empirical pseudopotential method, Wang *et al.*^{9,10} studied the influence of an external charge on the electron–hole pair in the spherical CdSe QD. The electron–hole interaction in Ref. 10 was averaged so that the exciton problem was reduced to two single particle problems. While this is a good approximation for the 4-nm-diam CdSe QDs, it is not acceptable for ZnO QDs of the same size. This difference comes from the fact that the exciton Bohr radius in ZnO is only 0.9

nm.¹¹ Since the size of ZnO QDs is only two to three times larger than the size of the exciton, the electron–hole interaction and quantum confinement effects have comparable strengths. Therefore, a two-particle problem has to be solved for an exciton in ZnO QDs.

The solution of a two-particle problem is a challenging task for atomistic tight-binding or pseudopotential methods. On the other hand, the multiband effective-mass method works surprisingly well for the description of lowest exciton states even for quantum shells as thin as one monolayer.¹² We employ the latter method to solve the six-dimensional exciton problem (it can be reduced to a five-dimensional one by making use of the axial symmetry of exciton wave functions along the *c* axis in wurtzite ZnO).

The exciton Hamiltonian with and without an ionized impurity present at the QD surface is written as

$$\hat{H}_{\text{exc}} = [\hat{H}_e + V_{s-a}(\mathbf{r}_e)] - [\hat{H}_h - V_{s-a}(\mathbf{r}_h)] + V_{\text{int}}(\mathbf{r}_e, \mathbf{r}_h) + \alpha(V_{\text{int}}(\mathbf{R}, \mathbf{r}_e) - V_{\text{int}}(\mathbf{R}, \mathbf{r}_h)), \quad (1)$$

where the two-band electron and the six-band hole Hamiltonians \hat{H}_e and \hat{H}_h for wurtzite nanocrystals have been introduced in Ref. 13. Since the dielectric constants of ZnO QD and of the exterior medium are different, the Coulomb potential energy of the electron–hole system in Eq. (1) is represented by the sum of the electron–hole interaction energy $V_{\text{int}}(\mathbf{r}_e, \mathbf{r}_h)$ and electron and hole self-interaction energies $V_{s-a}(\mathbf{r}_e)$ and $V_{s-a}(\mathbf{r}_h)$, which are calculated numerically after Ref. 14. In the last term of Eq. (1), \mathbf{R} is the radius-vector of the impurity and α is the charge of the impurity in units of $|e|$ ($\alpha=1$ for a donor, $\alpha=-1$ for an acceptor, and $\alpha=0$ when there is no impurity). The *z* axis is chosen to be parallel to the *c* axis of wurtzite ZnO. Therefore, we consider an impurity located on the *z* axis to keep the axial symmetry of the problem.

To calculate the exciton states we neglect the small penetration of the exciton wave function into the exterior medium and solve the Schrödinger equation with Hamiltonian (1) using the finite-difference method¹⁴ (a cubic grid with unit length of 0.05 nm has been used, which ensured the relative error for the exciton ground state energy $<1\%$). The following parameters of ZnO from Ref. 15 have been used: electron effective mass $m_e=0.24$; Rashba–Sheka–Pikus pa-

^{a)}Electronic mail: alexb@ee.ucr.edu

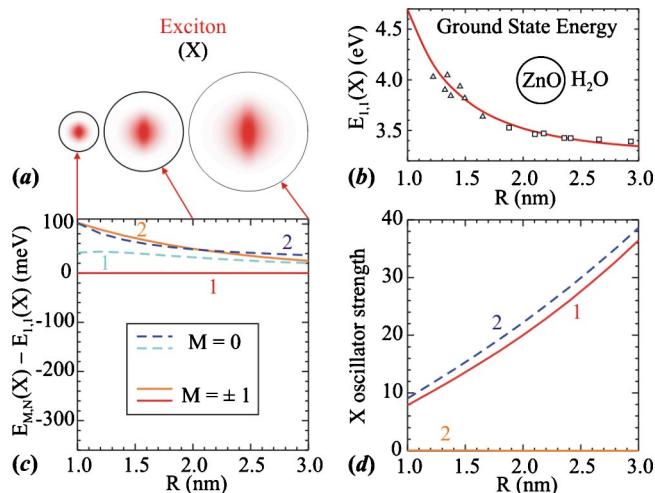


FIG. 1. (Color online). (a) Wave functions of exciton center of mass for three ZnO quantum dots with different sizes. (b) Calculated exciton ground state energy as a function of the quantum dot radius (ambient medium is water) and experimental points from Ref. 3 (boxes) and Ref. 7 (triangles). (c) Lowest exciton energy levels counted from the ground state energy. (d) Exciton oscillator strength as a function of the quantum dot radius. Solid (dashed) lines correspond to $|M|=1$ ($M=0$).

rameters A_1 – A_6 of the valence band are -3.78 , -0.44 , 3.45 , -1.63 , -1.68 , -2.23 , respectively, and $A_7=0.47$ nm $^{-1}$; crystal-field splitting energy $\Delta_{cr}=38$ meV; and dielectric constant $\epsilon=3.7$. The bulk band-gap energy of wurtzite ZnO is $E_g=3.437$ eV.¹⁶ A very small spin–orbit splitting, which is about 10 meV,^{15,16} has been neglected.

The results of our calculation for an exciton confined in spherical ZnO QD in water are shown in Fig. 1. It is seen from Fig. 1(a) that the wave function of the exciton ground state with equal electron and hole coordinates, i.e., the exciton center of mass, is prolate along the c axis of wurtzite ZnO. It is also seen that the thickness of the dead layer¹¹ increases with QD size. Note that the above-mentioned features, which have a strong influence on the optical properties, can be obtained only if the electron–hole interaction is taken into account exactly. Figure 1(b) shows calculated ground state energy of confined excitons as a function of the QD radius. As one can see, our theoretical results are in excellent agreement with experimental data reported in Refs. 3 and 7. If we consider ZnO QDs in air ($\epsilon=1$) instead of water ($\epsilon=1.78$), the exciton ground state energy slightly increases. The energy difference due to the change of the ambient (water \rightarrow air) decreases from 70 to 13 meV when the QD radius increases from 1 to 3 nm.

Due to the axial symmetry of the exciton problem, the z -component M of the exciton angular momentum is a good quantum number. The size dependence of the four lowest exciton energy levels with $|M|=0, 1$ is shown in Fig. 1(c) relative to the ground state energy, which has $M=\pm 1$. In an absorption spectrum, the intensity of an exciton state with energy E_{exc} and envelope wave function $\Psi_{exc}(\mathbf{r}_e, \mathbf{r}_h)$ is characterized by the oscillator strength:¹³

$$f = \frac{E_p}{E_{exc}} \left| \int_V \Psi_{exc}^{(\beta)}(\mathbf{r}, \mathbf{r}) d\mathbf{r} \right|^2, \quad (2)$$

where the Kane energy of ZnO is $E_p=28.2$ eV.¹¹ In Eq. (2) β denotes the component of the wave function, which is active for a given polarization. In the dipole approximation, only

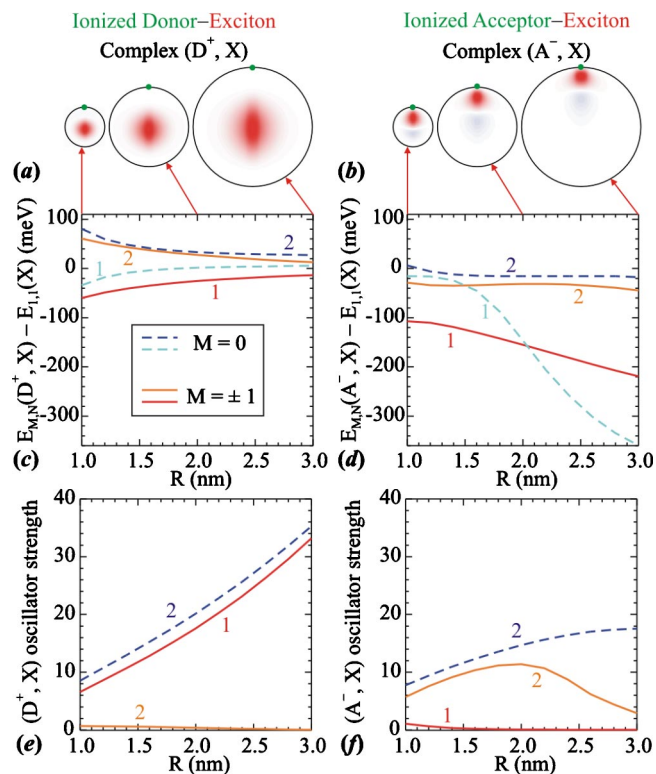


FIG. 2. (Color online). (a), (b) Wave functions of exciton center of mass for three ZnO quantum dots with different sizes. (c), (d) Lowest energy levels of ionized impurity–exciton complexes counted from the exciton ground state energy [see Fig. 1(b)]. (e), (f) Corresponding oscillator strengths as a function of the quantum dot radius. Panels (a), (c), (e) and (b), (d), (f) show the calculated results in the presence of an ionized donor and ionized acceptor, respectively. Large dots show the position of the impurity. Solid (dashed) lines correspond to $|M|=1$ ($M=0$).

exciton energy levels with $|M|=0, 1$ can be optically active, i.e., they can have a nonzero oscillator strength. Besides, the exciton energy levels with $M=0$ ($M=\pm 1$) are optically active only for the polarization $\mathbf{e} \parallel \mathbf{z}$ ($\mathbf{e} \perp \mathbf{z}$). Figure 1(d) shows the oscillator strengths of the exciton energy levels presented in Fig. 1(c). Note that the oscillator strength of the first energy level with $M=0$ is not shown; because it is found to be zero for all considered QD sizes.

Analogous to Fig. 1, calculated optical properties of ionized donor–exciton, and ionized acceptor–exciton complexes in spherical ZnO QDs are presented in Fig. 2. It is seen from Fig. 2(a) that the dead layer is observed near the QD surface for the ionized donor–exciton complex. On the contrary, Fig. 2(b) shows that the ionized acceptor–exciton complex is located in the vicinity of the acceptor. This means that the exciton is bound to the surface-located acceptor. Unlike the acceptor, the donor does not bind the exciton. Figures 2(c) and 2(d) show the size dependence of the four lowest exciton energy levels with $|M|=0, 1$ in the ZnO QDs with surface impurities. The energy levels are counted from the ground state energy of the confined exciton (no impurities). It is seen that the absolute value of the plotted energy difference for the donor–exciton complex is small and decreases with QD size, while this absolute value is much larger and increases with QD size for the acceptor–exciton complex. Such a different behavior of the exciton energy levels is due to the fact that the hole is much heavier than the electron, which makes the surface donor a shallow impurity, while the surface ac-

ceptor a deep impurity. Therefore, excitons can be effectively bound only to surface acceptors.

Figures 2(e) and 2(f) show the oscillator strengths of the exciton energy levels from Figs. 2(c) and 2(d). We can see that for the confined excitons and ionized donor–exciton complexes there are two energy levels that have large oscillator strengths (the first level with $|M|=1$ and the second level with $M=0$). The energy difference between the two energy levels decreases while their oscillator strengths, which are almost the same for both levels, increase with increasing the QD size. On the other hand, the oscillator strength of the ground state of the ionized acceptor–exciton complex is very small and decreases with QD size. Instead, the second energy level, with $|M|=1$, has large oscillator strength with a maximum for a QD with the radius of about 2 nm.

Summarizing the above noted observations, one can conclude that the absorption edge, which is defined by the first energy level with $|M|=1$ for the confined exciton and for the ionized donor–exciton complex and by the second energy level with $|M|=1$ for the ionized acceptor–exciton complex, depends on the presence of impurities relatively weakly and it is only few tens of milli electron volts lower in energy for the impurity–exciton complexes than it is for the confined excitons. On the contrary, the position of the UV photoluminescence peak, which is defined by the first energy level with $|M|=1$ for all considered cases, is 100–200 meV lower in energy for the ionized acceptor–exciton complex than it is for the confined exciton or the ionized donor–exciton complex. Most of the fabrication techniques, e.g., wet chemical synthesis,^{2,7} produce ZnO QDs, which have the position of the UV photoluminescence peak close to the absorption edge. We can attribute the UV photoluminescence in such QDs to confined excitons. The surface of such QDs may contain donors, which only slightly affect the UV photoluminescence. Other fabrication techniques, such as the wet chemical synthesis in the presence of a polymer,¹ produce ZnO QDs, which have the UV photoluminescence peak redshifted from the absorption edge as far as a few hundreds of milli electron volts. We argue that this redshift may be caused by the presence of acceptors at the surface of ZnO QDs. The ionized acceptors, e.g., $(\text{NaO})^-$, are more likely to be at the QD surface than inside the QD, because the latter fabrication techniques include some type of surface passivation. For example, the method described in Ref. 1 produces ZnO QDs capped with the polyvinyl pyrrolidone (PVP) polymer.

In the following, we suggest that the presence of acceptors at the surface of ZnO QDs can be determined by measuring the exciton radiative lifetime. The radiative recombination lifetime τ of excitons in bulk ZnO is about 322 ps.¹⁷ In low-dimensional structures, such as QDs, the radiative lifetime can be calculated as¹³

$$\tau = \frac{2\pi\epsilon_0 m_0 c^3 \hbar^2}{\sqrt{\epsilon} e^2 E_{exc}^2 f}, \quad (3)$$

where f is the oscillator strength (2) and all other parameters have been defined earlier or they are universal physical constants. It has been established that the lifetime of confined excitons is less than 50 ps for QDs with diameter 5 nm.² Figure 3 shows the radiative lifetime as the function of the QD radius for the confined excitons as well as for the

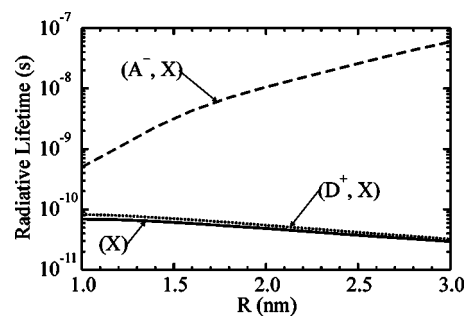


FIG. 3. Radiative lifetime of confined excitons (solid line) and ionized impurity–exciton complexes (dotted and dashed lines) for ZnO quantum dots as a function of the quantum dot radius.

impurity–exciton complexes. It is seen that the radiative lifetime of the confined exciton and that of the ionized donor–exciton complex are almost the same; they decrease with QD size and are about an order of magnitude less (for $R \sim 2$ nm) than the bulk exciton lifetime. For the QD with diameter 5 nm we get the lifetime of 38 ps, in agreement with the conclusion of Ref. 2. On the other hand, the radiative lifetime of the ionized acceptor–exciton complex increases with QD size very fast and it is about two orders of magnitude larger (for $R \sim 2$ nm) than bulk exciton lifetime.

In conclusion, we have found that, depending on the fabrication technique and ZnO QD surface quality, the origin of UV photoluminescence in ZnO QDs is either recombination of confined excitons or surface-bound ionized acceptor–exciton complexes. In the latter case the Stokes shift of the order of 100–200 meV should be observed in the photoluminescence spectrum. We have also proposed to use the exciton radiative lifetime as a probe of the exciton localization.

The authors acknowledge the financial and program support of the Microelectronics Advanced Research Corporation (MARCO) and its Focus Center on Functional Engineered Nano Architectonics (FENA). The work was also supported in part by the ONR Young Investigator Award to A.A.B. and NSF-NATO 2003 award to V.A.F.

¹L. Guo, S. Yang, C. Yang, P. Yu, J. Wang, W. Ge, and G. K. L. Wong, Appl. Phys. Lett. **76**, 2901 (2000).

²D. W. Bahnemann, C. Kormann, and M. R. Hoffmann, J. Phys. Chem. **91**, 3789 (1987).

³E. A. Muelenkamp, J. Phys. Chem. B **102**, 5566 (1998).

⁴S. Mahamuni, K. Borgohain, B. S. Bendre, V. J. Leppert, and S. H. Risbud, J. Appl. Phys. **85**, 2861 (1999).

⁵E. M. Wong and P. C. Searson, Appl. Phys. Lett. **74**, 2939 (1999).

⁶A. Dijken, E. A. Muelenkamp, D. Vanmaekelbergh, and A. Meijerink, J. Phys. Chem. B **104**, 1715 (2000).

⁷A. Wood, M. Giersig, M. Hilgendorff, A. Vilas-Campos, L. M. Liz-Marzan, and P. Mulvaney, Aust. J. Chem. **56**, 1051 (2003).

⁸H. Zhou, H. Alves, D. M. Hofmann, W. Kriegseis, B. K. Meyer, G. Kaczmarczyk, and A. Hoffmann, Appl. Phys. Lett. **80**, 210 (2002).

⁹L. W. Wang and A. Zunger, Phys. Rev. B **53**, 9579 (1996).

¹⁰L. W. Wang, J. Phys. Chem. B **105**, 2360 (2001).

¹¹V. A. Fonoberov and A. A. Balandin, Phys. Rev. B **70**, 195410 (2004).

¹²V. A. Fonoberov, E. P. Pokatilov, V. M. Fomin, and J. T. Devreese, Phys. Rev. Lett. **92**, 127402 (2004).

¹³V. A. Fonoberov and A. A. Balandin, J. Appl. Phys. **94**, 7178 (2003).

¹⁴V. A. Fonoberov, E. P. Pokatilov, and A. A. Balandin, Phys. Rev. B **66**, 085310 (2002).

¹⁵W. R. L. Lambrecht, A. V. Rodina, S. Limpijumng, B. Segall, and B. K. Meyer, Phys. Rev. B **65**, 075207 (2002).

¹⁶D. C. Reynolds, D. C. Look, B. Jogai, C. W. Litton, G. Cantwell, and W. C. Harsch, Phys. Rev. B **60**, 2340 (1999).

¹⁷D. C. Reynolds, D. C. Look, B. Jogai, J. E. Hoelscher, R. E. Sherriff, M. T. Harris, and M. J. Callahan, J. Appl. Phys. **88**, 2152 (2000).